Monatsh Chem (2011) 142:45–52
DOI 10.1007/s00706-010-0424-z

ORIGINAL PAPER

Density functional theory as a guide for the design of pyran dyes for dye-sensitized solar cells

Christopher Johnson · Seth B. Darling · Youngjae You

Received: 3 June 2010 / Accepted: 8 November 2010 / Published online: 8 December 2010

Abstract Using density functional theory and hybrids, we examined several derivatives of the dye 4-(dicyanomethylene)-2-methyl-6-(*p*-dimethylaminostyryl)-4*H*-pyran, with the objective of identifying modifications which would improve the properties of dyes for dye-sensitized solar cells. We calculated the electronic structure of numerous derivatives at the HOMO and LUMO energy levels, with the hypothesis that directing the flow of excited electrons to the point of the dye at which the molecule attaches to TiO_2 would increase the energy conversion efficiency of the cell. We also examined the UV–visible absorption spectra of the dyes, with the objective of capturing the maximum amount of solar light. By use of the derivatives we compared the use of two electron-donating groups instead of one, extension of the conjugated chain leading to the attachment point of the dye, use of oxygen versus sulfur or selenium in the dye, and the use of different electron-donating groups. We identified several promising donating groups and determined that the other modifications to the dye are likely to increase solar cell efficiency.

Keywords Absorption spectra · Computational chemistry · Dyes · Electronic structure · Orbitals

C. Johnson · Y. You (✉)
Department of Chemistry and Biochemistry,
South Dakota State University, Brookings, SD 57007, USA
e-mail: youngjae.you@sdstate.edu

S. B. Darling
Argonne National Laboratory, Center for Nanoscale Materials,
9700 S Cass Ave, Argonne, IL 60439-4806, USA

Introduction

Dye-sensitized solar cells (DSSCs) have been undergoing research as a possible alternative to current silicon solar cells, which are expensive to produce [1, 2]. In DSSCs photons are absorbed by a dye, exciting electrons in the dye from their HOMO to LUMO energy level. These electrons are then passed to a TiO_2 layer, after which they are used to generate electricity in an external circuit. They are then passed to iodide/triiodide electrolyte, which returns the electrons to the dye to repeat the cycle (Fig. 1) [3].

Ruthenium dye-based DSSCs have proved capable of achieving efficiency of ten to eleven percent [4]. These dyes have the advantages of tending to be more stable than purely organic dyes, with less of a tendency to aggregate, and higher conversion yields [2, 5]. However, the rarity of Ru is such that it would be costly to mass-produce cells based on these dyes [6], and there are environmental concerns with the widespread use of heavy metals. Consequently, there have been efforts to develop efficient dyes without heavy metals, for example coumarin [7, 8], squaraine [9, 10], inoline [11, 12], porphyrin [13], and cyanine-based dyes [6]. These organic dyes have advantages in the form of higher absorption coefficients, more easily manipulated HOMO and LUMO energy levels, and the aforementioned advantage of cost, although they are at times not as stable as metal-based dyes and have yet to achieve the same efficiency [6].

Density functional theory (DFT) and hybrid calculations have been used to investigate the electronic properties of dyes for DSSCs [14–19]. These calculations are capable of predicting three important characteristics of dyes: the electron density distribution in both the ground and excited states in a molecule, energy levels of frontier molecular orbitals, and UV–visible spectra. Various results from these

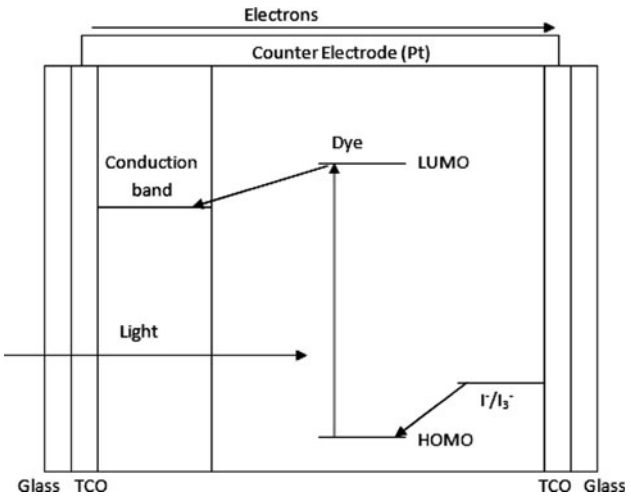

Fig. 1 Electron flow within DSSC: electrons flow in a functioning dye-sensitized solar cell, using relative energy levels for transitions (modified from Ref. [3])

calculations can provide indications of performance in a solar cell. In the context of electronic structure, vectorial momentum of photoexcited electrons in the dye toward the electron-accepting TiO_2 nanoparticle may improve effectiveness of charge carrier flow in the cells. Looking at the frontier orbital energies, the LUMO energy level should be sufficiently higher than the TiO_2 conduction band for electron injection and the HOMO should be sufficiently lower than the redox potential of the I^-/I_3^- to be readily reduced. Light harvesting, as modeled by absorption spectra, is related to the potential quantity of electrons that can be excited, therefore providing insight into the overall efficiency of the cell. In designing new dyes for DSSCs, these simulated data will be particularly valuable, because of the prospect of identifying promising synthetic targets and thereby requiring significantly less experimental effort.

In this project, we systemically designed a virtual dye ensemble. The derivatives in the virtual library have the following structural features (Fig. 2; Table 1):

1. one or two electron-donating groups;
2. various chalcogenic atoms (X = O, S, or Se) at the ring between donor and acceptor groups;
3. extended conjugated chain length (n = 0–1); and
4. various electron-donating groups.

We then calculated the UV–visible absorption spectra of these dyes using time-dependent DFT and examined qualitative structural effects on these spectra. The objective was to identify the broadest range of absorbance, including maximum red-shift, given the tendency of DSSCs to attain greater absorbance in blue-shifted wavelengths upon aggregation [8, 10, 20]. We also calculated the electronic structure and energy levels of the frontier molecular

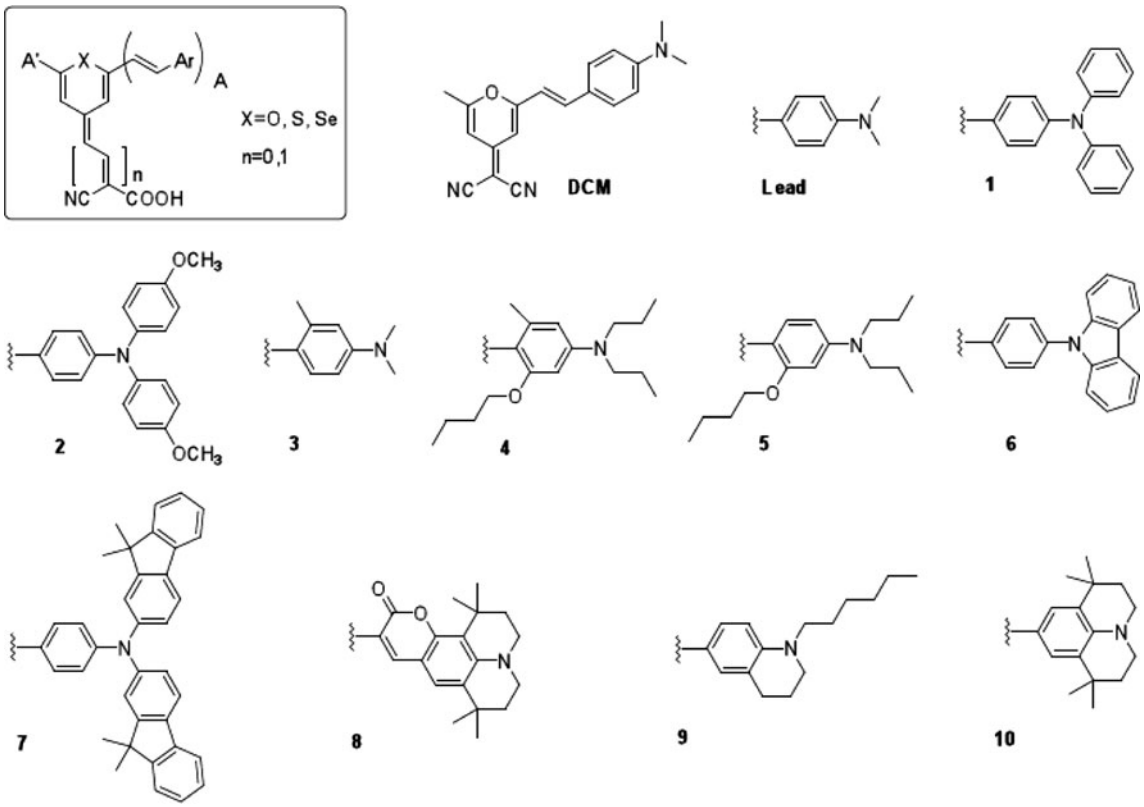

Fig. 2 DCM and proposed modifications: the proposed modifications to the dye (*top left*), DCM, and the alternative donating (Ar) groups

Table 1 Structures of dyes: configuration of calculated dyes, using terminology from Fig. 2

Molecule	Ar	X	A′	*n*	Molecule	Ar	X	A′	*n*
DL-O	Lead	O	Me	0	D4-Se	4	Se	Me	0
DL-S	Lead	S	Me	0	D5-O	5	O	Me	0
DL-Se	Lead	Se	Me	0	D5-S	5	S	Me	0
DL-O-DL	Lead	O	A	0	D5-Se	5	Se	Me	0
DL-S-DL	Lead	S	A	0	D6-O	6	O	Me	0
DL-Se-DL	Lead	Se	A	0	D6-S	6	S	Me	0
DL-O-E	Lead	O	Me	1	D6-Se	6	Se	Me	0
DL-S-E	Lead	S	Me	1	D7-O	7	O	Me	0
DL-Se-E	Lead	Se	Me	1	D7-S	7	S	Me	0
D1-O	1	O	Me	0	D7-Se	7	Se	Me	0
D1-S	1	S	Me	0	D8-O	8	O	Me	0
D1-Se	1	Se	Me	0	D8-S	8	S	Me	0
D2-O	2	O	Me	0	D8-Se	8	Se	Me	0
D2-S	2	S	Me	0	D9-O	9	O	Me	0
D2-Se	2	Se	Me	0	D9-S	9	S	Me	0
D3-O	3	O	Me	0	D9-Se	9	Se	Me	0
D3-S	3	S	Me	0	D10-O	10	O	Me	0
D3-Se	3	Se	Me	0	D10-Se	10	S	Me	0
D4-O	4	O	Me	0	D10-Se	10	Se	Me	0
D4-S	4	S	Me	0					

orbitals. Effects of structural modifications were examined qualitatively, in particular, on UV–visible spectra and electron-density maps.

Results and discussion

Calculation accuracy

Before analyzing the computational results, it is important to identify the overall accuracy of the calculations. Geometries of small organic molecules are typically reproduced reasonably accurately with the B3LYP functional and the 3-21G* basis set, with larger bases typically producing similar results and hence unnecessarily taxing computational resources. However, larger basis sets are often necessary to capture even qualitatively correct electronic structure or absorption properties.

Although experimental data are not available for the various novel dye molecules investigated here, data for 4-(dicyanomethylene)-2-methyl-6-(*p*-dimethylaminostyryl)-4*H*-pyran (DCM) are available in the literature [21]. In this baseline experiment, DCM-TPA was compared with DCM and DCM 2 to analyze the effects of charge trapping and its effects on fluorescence, with the objective of creating a dye to be used in organic light-emitting diodes. Of particular use, the experimental HOMO and LUMO values of each derivative were taken for each of the versions reported, giving us a baseline upon which we could judge the accuracy of our calculations.

The calculated HOMO and LUMO energies (Table 2), which have not been adjusted with any scaling factor, were

Table 2 Calculated HOMO and LUMO energies (eV) of each molecule

Molecule	HOMO	LUMO	Gap
DL-O	−5.48	−2.49	2.99
DL-S	−5.42	−2.63	2.79
DL-Se	−5.46	−2.73	2.73
DL-O-DL	−5.32	−2.49	2.83
DL-S-DL	−5.28	−2.66	2.62
DL-Se-DL	−5.27	−2.73	2.55
DL-O-DL	−5.44	−2.72	2.72
DL-S-DL	−5.44	−2.89	2.55
DL-Se-DL	−5.44	−2.96	2.48
D1-O	−5.50	−2.70	2.79
D1-S	−5.44	−2.79	2.65
D1-Se	−5.47	−2.94	2.53
D2-O	−4.99	−2.43	2.56
D2-S	−5.23	−2.69	2.54
D2-Se	−5.47	−2.94	2.53
D3-O	−5.43	−2.54	2.89
D3-S	−5.41	−2.67	2.74
D3-Se	−5.36	−2.70	2.65
D4-O	−5.24	−2.29	2.95
D4-S	−5.27	−2.51	2.77
D4-Se	−5.67	−2.75	2.92
D5-O	−5.30	−2.32	2.98
D5-S	−5.32	−2.53	2.79
D5-Se	−5.30	−2.60	2.70
D6-O	−5.82	−2.97	2.85
D6-S	−5.78	−3.03	2.75
D6-Se	−5.77	−3.09	2.68
D7-O	−5.29	−2.69	2.59
D7-S	−5.26	−2.87	2.39
D7-Se	−5.26	−2.93	2.33
D8-O	−5.52	−2.71	2.81
D8-S	−5.48	−2.75	2.73
D8-Se	−5.46	−2.79	2.67
D9-O	−5.32	−2.47	2.86
D9-S	−5.32	−2.67	2.65
D9-Se	−5.32	−2.74	2.58
D10-O	−5.22	−2.36	2.86
D10-S	−5.23	−2.52	2.71
D10-Se	−5.24	−2.71	2.53
DCM	−5.55	−2.58	2.97

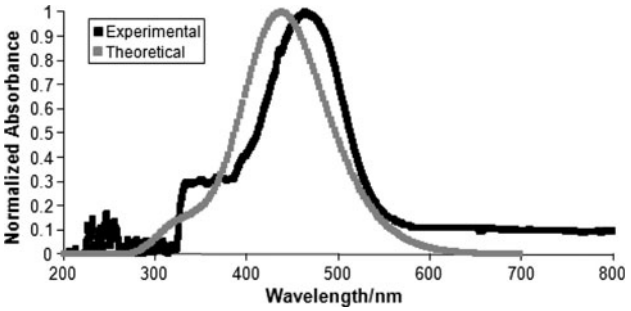

Fig. 3 Calculation-based and experimental UV–visible spectra of DCM: comparison of experimental and B3LYP/6-311G(d,p) UV–visible spectra

also compared with experimentally derived values. The calculated HOMO energy (−5.55 eV) was remarkably similar to the experimental value (−5.56 eV), the calculated value being only 0.01 eV higher [21]. The calculated LUMO energy (−2.58 eV), however, was 0.85 eV higher than the experimental value (−3.43 eV). Therefore, the quantitative LUMO results presented here should be assessed for trends rather than precise prediction of the band gap. That said, the conduction band of TiO_2 (−4.2 eV) is over 1.1 eV lower than the LUMO energies of any of the modeled dyes (the lowest LUMO, −3.09 eV of D6-Se), meaning that this margin of error should not play a role that would impede electron transfer to the conduction band of TiO_2 (Fig. 1).

The experimental UV–visible spectrum of DCM was obtained in our laboratory. Comparing the UV–visible spectrum for DCM with the calculated spectrum, the general shape is indeed similar, although approximately 20 nm red-shifted from the experimental spectrum (Fig. 3). For the purposes of the comparisons discussed here, this shift is not a major issue, particularly given that the same calculation methodology was used for all theoretical molecules, and it is sufficiently close to experimental results.

Substitution of oxygen with sulfur and selenium

With a sense of the reliability of the calculations determined, we now turn to the results of the calculations. The first modification to consider is substitution of the atom in the six-membered ring. Sulfur and selenium were chosen because these are heavier than oxygen in the same Group 16 having two covalent bonds. Compounds with sulfur and selenium seemed quite stable to oxidation by singlet

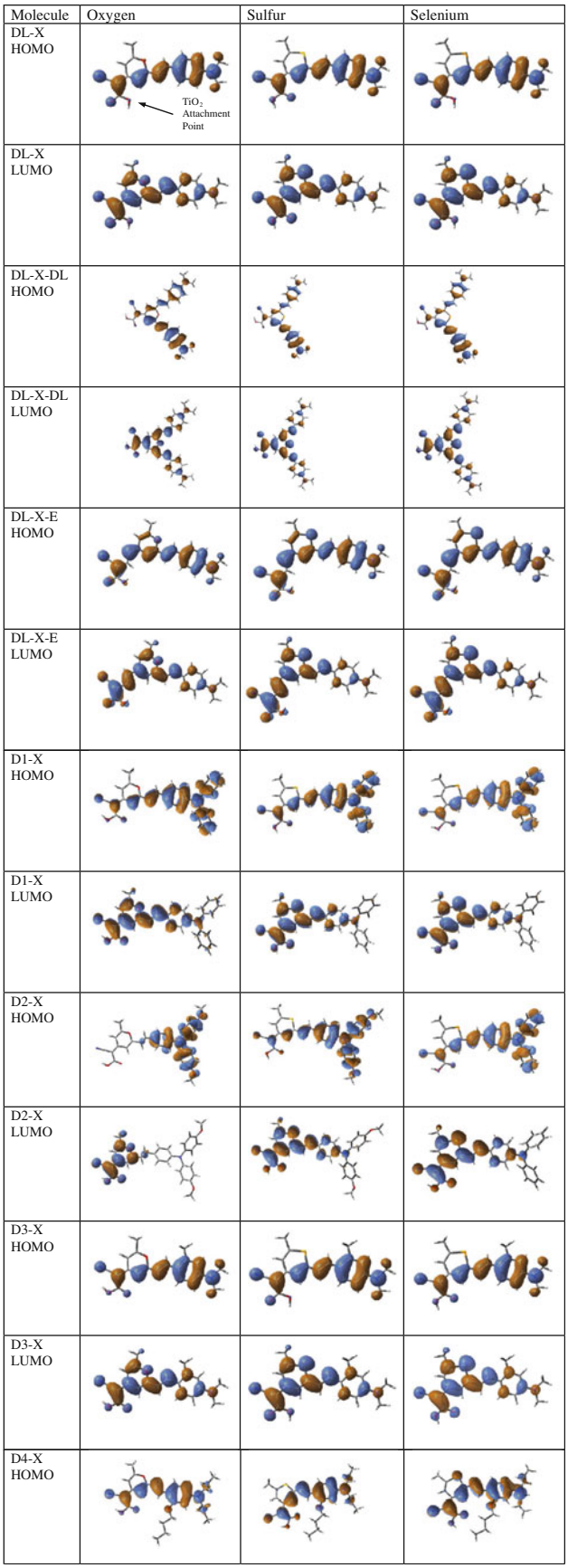

Fig. 4 HOMO and LUMO electronic structure of proposed dyes: the calculated effect of dye modification on electron flow, with the attachment point of the dye to the TiO_2 layer labeled in the lead molecule's oxygen version HOMO image ▶

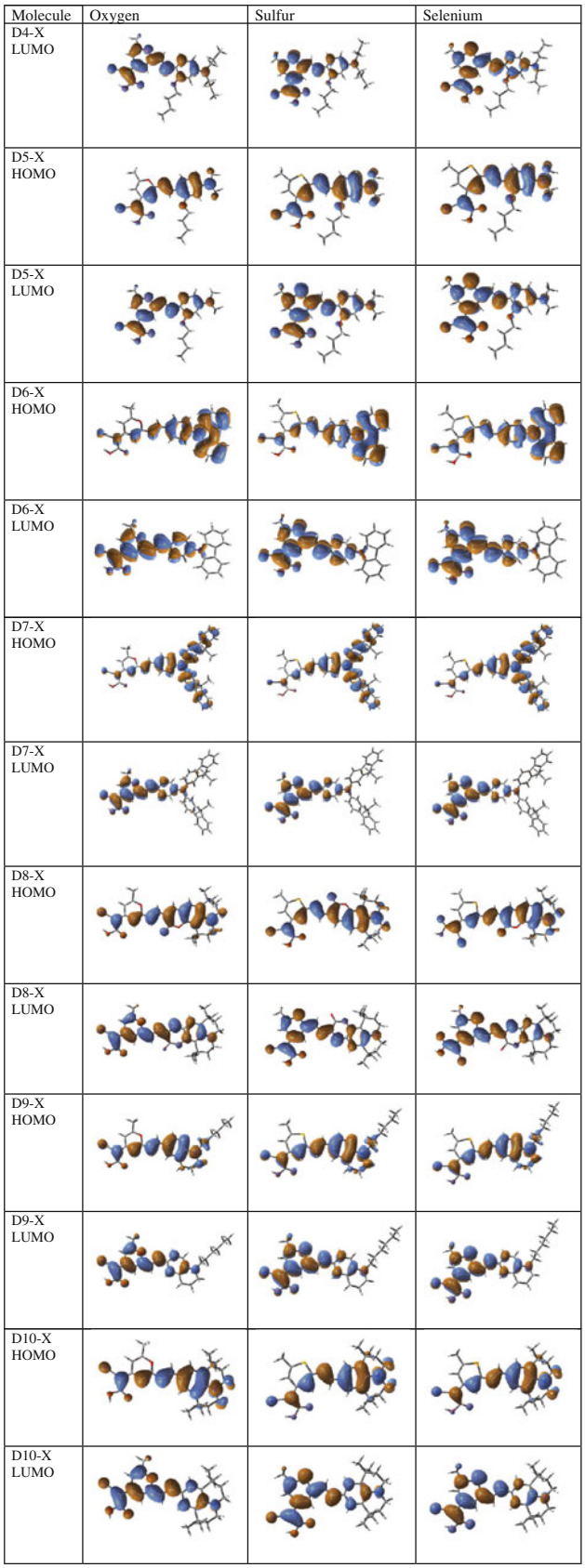

Fig. 4 continued

oxygen compared with that with tellurium [22]. Substitution of oxygen with these atoms lowered the band gap of the compounds [22–24]. Replacement of oxygen with sulfur or selenium generally resulted in greater spatial localization of the electrons in the frontier molecular orbitals, with the electrons congregating more strongly towards the electron-donating group at the HOMO level and the attachment point at the LUMO level as the replaced atom increased in size (Fig. 4). This would help to guide the electrons into the titanium dioxide layer and the rest of the cell, where they would be of use in electricity generation. Furthermore, the replacement of oxygen tends to red-shift the absorption peaks, with a usual red-shift of 30–40 nm between oxygen and sulfur or selenium, although the specific red-shift varies somewhat among the different donating groups (Fig. 5). As stated above, because higher wavelengths are not covered by aggregation effects, this would enable the cell to access a broader spectrum of light, thus capturing more of the available light energy and exciting more electrons, which can then be used to generate electricity.

Interestingly, when donating group 2 was used (Fig. 2), the effect of sulfur and selenium was reversed with regard to electron polarization, which was highly localized using oxygen and less localized with sulfur and selenium. For the purposes of facilitating electron transfer to the oxide via the attachment point, greater localization as described above is encouraging. The trend of improvement by replacing oxygen with sulfur or selenium was observed for all but one of the donating groups, indicating that the substitution seems sufficiently promising to warrant synthesis.

Multiple electron-donating groups

DCM has one electron-donating group, as do most of the alternative moieties investigated here. In order to probe the effect of having an additional donor, calculations were performed for a set of molecules in which there were two lead donating groups. On the basis of the electronic structure of the frontier orbitals, it seems that use of two electron-donating groups instead of one had little effect on electron flow. This would, therefore, not aid the transfer of electrons into the main cell, but nor do the additional groups seem to prevent electron transfer. However, this modification red-shifted the absorption peak maximum by approximately 40 nm (DL-O vs. DL-O-DL, Fig. 5), increasing the net amount of light absorbed and the number of electrons excited to do work. Similarly, the extension of the conjugated chain at the attachment point had little effect on the electron flow, but resulted in an approximately 20–40 nm red-shift of the major peak (DL-O vs. DL-O-E, Fig. 5). As a narrower band gap between the

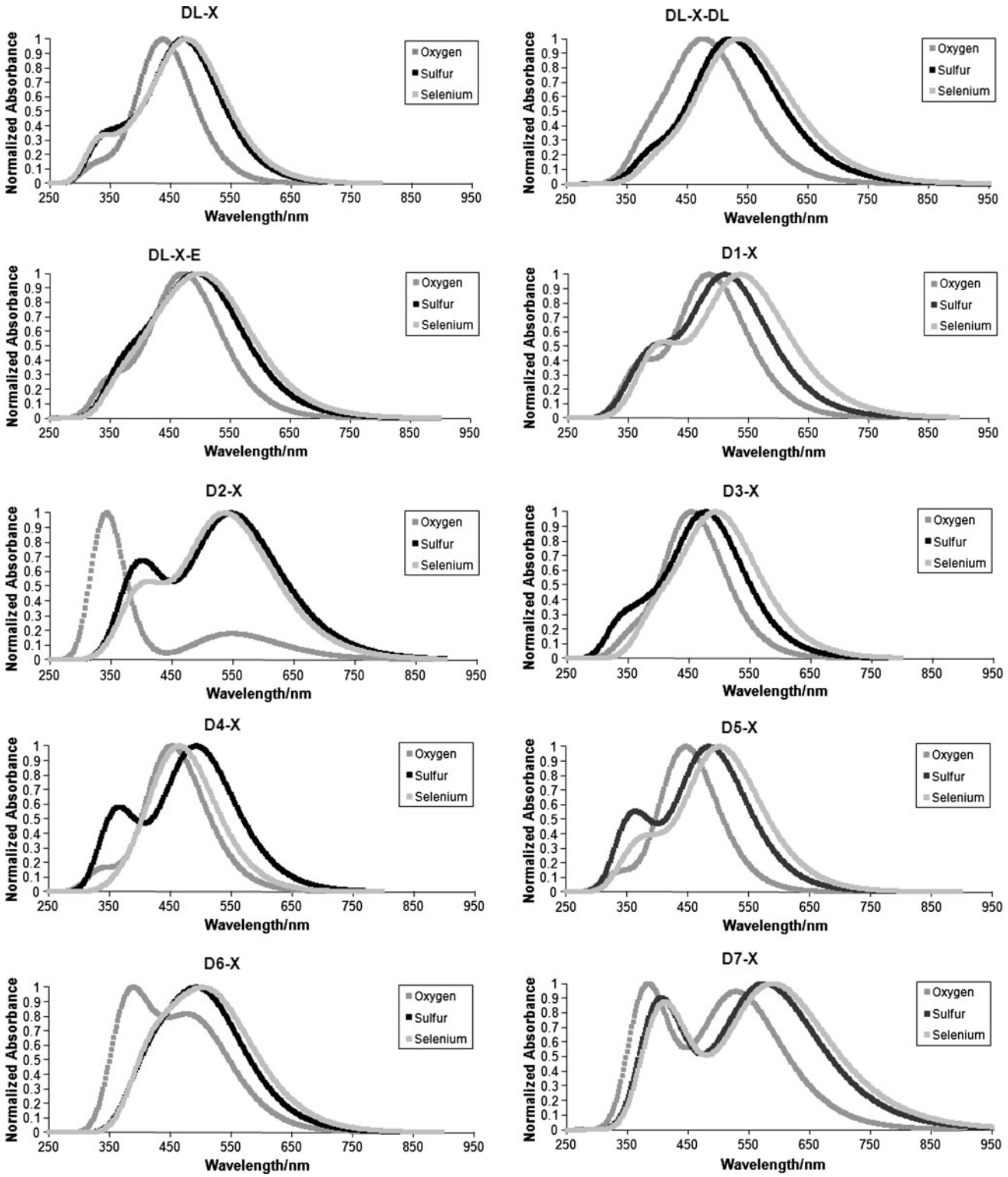

Fig. 5 UV–visible comparison: the UV–visible spectra of the lead molecule with each alternative donating group, extended conjugation, and the use of two donating groups. Oxygen, sulfur, and selenium variants are shown for each donating group

HOMO and LUMO energies generally results in a red-shift of the absorption spectrum, a phenomenon which occurred when these modifications were made, it is likely that this is responsible for the red-shift observed in the simulated spectra (DL-O vs. D1-O, Table 1; Fig. 5). As stated above, extension of absorption further into the red is advantageous

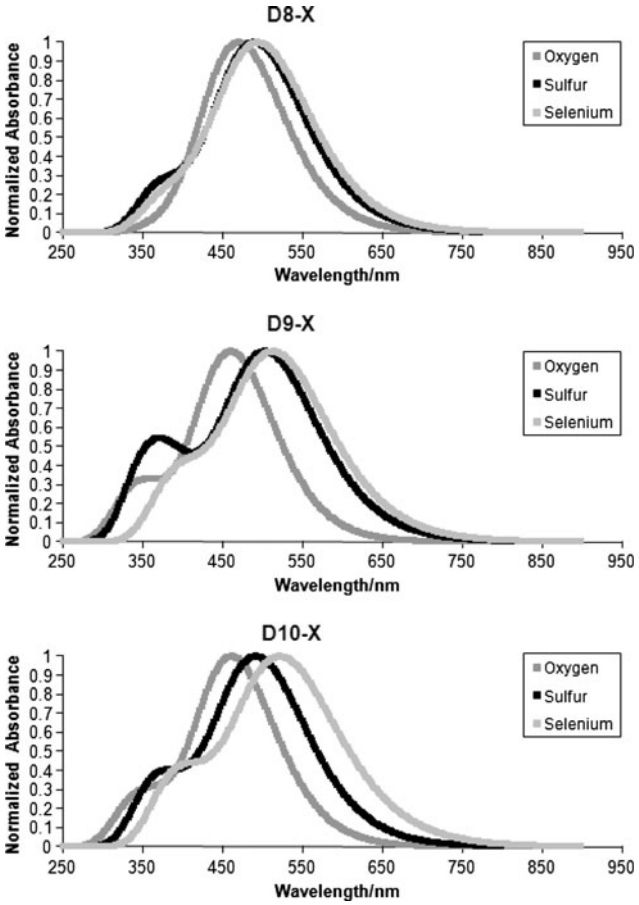

Fig. 5 continued

for light harvesting, making both modifications promising candidates for synthesis.

Alternative electron-donating groups

Focusing on use of a single electron-donating group, a variety of alternative chemistry was explored. Of the replacement electron-donating groups tested, the most promising were groups 1, 2, and 7 (Fig. 2). Aside from these three, most of the donating groups had a red-shift from the lead group of approximately 20–40 nm and a full width, half-maximum (FWHM) of their absorption peaks of approximately 150 nm. In contrast, group 2 had the second largest red-shift, at about 70 nm in its sulfur and selenium versions, and had the second broadest absorbance of the donating groups, with an FWHM of 250 nm (Fig. 5); this means that not only was more light absorbed by virtue of the absorbance being in a region where less light is absorbed because of aggregation, but that more light was absorbed by the dye in general, which would cause more electrons to be excited and to potentially do work in the cell. Note that D2-O was the exception here; its HOMO energy level was calculated to be higher than the redox energy of iodine, potentially disrupting the transfer of electrons from iodine to the dye to be re-used in the cell, although this difference was small enough to be within the error range indicated for the HOMO energy level. It also did not have the same red-shift as the other two versions. Regardless, this dye molecule also had a strong electron flow which represents the most promising opportunity to test our hypothesis that increased electron flow to the TiO_2 attachment point would increase dye efficiency (Fig. 4).

Group 1 had no significant red shift (Fig. 5); however, it was calculated to have pronounced electron flow, meaning it would also be a useful candidate for testing the hypothesis that electron momentum toward the TiO_2 attachment point because of orbital localization can be used to enhance charge transfer.

For group 7 electron redistribution was not as complete an for groups 1 or 2, but it still had pronounced transfer of electrons to the parts of the molecule near the TiO_2 attachment point (Fig. 4), meaning that it should still be capable of guiding electrons into the rest of the cell. However, it had the greatest red shift of the three groups (100 nm), had strong absorption at shorter wavelengths and at long wavelengths, and absorbed strongly over a wider range of wavelengths than any other donating group, with an FWHM of approximately 300 nm (Fig. 5). This means that, in terms of the amount of light absorbed being converted into electricity, both in general and in covering the red-shifted regions, this is our most promising candidate. As a result, these three, in addition to the lead compound, are being synthesized and studied experimentally as part of ongoing work.

Conclusion

Of the modifications tested, replacement of the electron-donating groups showed the most variability. For electron-donating groups 1, 2, and 7, in particular, computational results indicated promise in increasing the solar cell efficiency by guiding electrons to the TiO_2 attachment point, channeling them into the cell where they can be used to generate electricity, and, in the case of 2 and 7, absorbing light which formerly could not have been utilized by the cell for electron excitation. Similarly, use of sulfur and selenium was calculated to affect both absorption wavelength and electron flow in such a way that they would, in most cases, improve the efficiency of the cell as compared with oxygen. Finally, both extension of the conjugated carbon chain leading to the point of attachment of the dye to TiO_2 and use of two electron-donating groups seem to increase light absorption wavelengths not covered by aggregation without significantly impairing electron flow.

These modifications therefore warrant synthesis and testing in experimental solar cells in order to determine the effect of the dye modifications on the percentage efficiency of the cell.

These calculations can be used to guide molecular design of DSSCs without having to physically synthesize each molecule. By rapidly assessing multiple chemical structures, calculations such as those performed here have the potential to save a great deal of effort that would normally be spent synthesizing and testing modifications, some of which would have negligible or deleterious effects on the cell. This will enable time to be spent on molecules which have greater potential.

Computational methods

Calculations were all performed using the commercial software package Gaussian03. Geometries of the various dye molecules were optimized by energy minimization using ground state B3LYP/3-21G* calculations, known to be reasonably accurate for molecules with application to photovoltaics [25]. Several of the molecules were also optimized using larger bases for comparison, and there were no dramatic changes in the atomic positions. Eigenvalues from frequency calculations performed on several representative molecules were all positive, confirming that the structures represent true energetic minima. Using the geometries produced by the optimizations, the UV–visible absorption spectra were then calculated using time-dependent self-consistent field methods at the B3LYP/6-311G(d,p) level with tight convergence criteria. The molecular orbital structures and energies were also calculated at the B3LYP/6-311G(d,p) level for both the highest occupied molecular orbital (HOMO) and lowest unoccupied molecular orbital (LUMO). The same set of calculations was applied to DCM; to assess the accuracy of our calculations the results were compared with experimental data reported in literature for this molecule and supplemented by cyclic voltammetry of DCM conducted in our laboratory.

Acknowledgments This material is based upon work supported by the National Science Foundation/EPSCoR Grant No. 0554609 and by the State of South Dakota. Use of the Center for Nanoscale Materials was supported by the US Department of Energy, Office of Science, Office of Basic Energy Sciences, under Contract No. DE-AC02-06CH11357. This material is based on work supported by the NASA South Dakota Space Grant Consortium.

References

1. O'Regan B, Graetzel M (1991) Nature 353:737
2. Grätzel M (2004) J Photochem Photobiol A 164:3
3. Hara K, Arakawa H (2003) Dye-sensitized solar cells. In: Luque A, Hegedus S (eds) Handbook of photovoltaic science and engineering. Wiley, New York
4. Kroon JM, Bakker NJ, Smit HJP, Liska P, Thampi KR, Wang P, Zakeeruddin SM, Grätzel M, Hinsch A, Hore S, Würfel U, Sastrawan R, Durrant JR, Palomares E, Pettersson H, Gruszecki T, Walter J, Skupien K, Tulloch GE (2007) Prog Photovolt Res Appl 15:1
5. Xie P, Guo F (2007) Curr Org Chem 11:1272
6. Chen Z, Li F, Huang C (2007) Curr Org Chem 11:1241
7. Wang ZS, Hara K, Danoh Y, Kasada C, Shinpo A, Suga S, Arakawa H, Sugihara H (2005) J Phys Chem B 109:3907
8. Wang ZS, Cui Y, Hara K, Dan-oh Y, Kasada C, Shinpo A (2007) Adv Mater 19:1138
9. Alex S, Santhosh U, Das S (2005) J Photochem Photobiol A 172:63
10. Burke A, Schmidt-Mende L, Ito S, Gratzel M (2007) Chem Commun 234
11. Howie WH, Claeyssens F, Miura H, Peter Laurence M (2008) J Am Chem Soc 130:1367
12. Horiuchi T, Miura H, Sumioka K, Uchida S (2004) J Am Chem Soc 126:12218
13. Campbell WM, Burrell AK, Officer DL, Jolley KW (2004) Coord Chem Rev 248:1363
14. Walsh PJ, Gordon KC, Officer DL, Campbell WM (2006) J Mol Struct (THEOCHEM) 759:17
15. Vyas S, Hadad CM, Modarelli DA (2008) J Phys Chem A 112:6533
16. Balanay MP, Kim DH (2008) Phys Chem Chem Phys 10:5121
17. Liu T, Zhang HX, Zhou X, Xia BH (2008) Eur J Inorg Chem 2008:1268
18. Liu Z (2008) J Mol Struct (THEOCHEM) 862:44
19. Balanay MP, Kim DH (2009) J Mol Struct (THEOCHEM) 910:20
20. Mann JR, Gannon MK, Fitzgibbons TC, Detty MR, Watson DF (2008) J Phys Chem C 112:13057
21. Nueesch F, Zuppiroli L, Berner D, Ma C, Wang X, Cao Y, Zhang B (2004) Res Chem Intermed 30:495
22. Detty MR, Merkel PB (1990) J Am Chem Soc 112:3845
23. Mautner HG, Clayton EM (1959) J Am Chem Soc 81:6270
24. Ohulchanskyy TY, Donnelly DJ, Detty MR, Prasad PN (2004) J Phys Chem B 108:8668
25. Darling SB (2008) J Phys Chem B 112:8891